

Nb₃Sn CRITICAL-CURRENT MEASUREMENTS USING TUBULAR FIBERGLASS-EPOXY MANDRELS
 L. F. Goodrich, S. L. Bray, and T. C. Stauffer
 National Bureau of Standards
 Boulder, Colorado 80303

Abstract

A systematic study of the effect of sample mounting techniques on the superconducting critical-current measurement was made in conjunction with the VAMAS (Versailles Agreement on Advanced Materials and Standards) interlaboratory comparison (round robin) measurements. A seemingly small change in mandrel geometry can result in a 40% change in the measured critical current of a Nb₃Sn sample at 12 T. This is a result of a change in the conductor pre-strain at 4 K caused by variation in thermal contraction between thick- and thin-walled fiberglass-epoxy composite (G-10) tubes. An approximate measure of the variations in thermal contraction (from room to liquid nitrogen temperature) indicate a 0.2% greater contraction for the thick-walled tube. This difference, combined with strain sensitivity measurements, is consistent with the observed decrease in critical current. Previous publications on the thermal contraction of G-10 have addressed the plate geometry, but not the tube geometry. The contraction of a G-10 plate is highly anisotropic. The radial contraction of a tube is different than the contraction of a plate, however, because the circumferential fiberglass is put into hoop compression by the epoxy, and the resulting contraction is a competition between the two structural components. This appears to be the source of the variation in thermal contraction with tube wall thickness.

Introduction

The measurements reported here are part of a collaborative effort involving twenty-four laboratories from the European Economic Community, Japan, and the USA under the Versailles Agreement on Advanced Materials and Standards (VAMAS). The purpose is to develop critical-current (I_c) measurement techniques for Nb₃Sn superconductors that will yield consistent results at different laboratories. Comparisons of preliminary results showed a large variation in the measured I_c . In response, the NBS study was expanded to address specific measurement variables that might have caused these discrepancies.

The predominant variables that affect I_c measurements of Nb₃Sn wires^{1,2} fall into four categories: sample reaction conditions, measurement mandrel (sample holder) material and geometry, the method used for bonding the sample to its mandrel, and damage incurred during shipping or in transferring the sample from the reaction mandrel (tubular stainless steel sample holder) to the measurement mandrel. In the last three categories, the sensitivity of Nb₃Sn to mechanical strain results in variations in the measured I_c .³ For these measurements, similar samples were reacted at a central location under (presumably) the same conditions; consequently, the reaction variables were not suspected of being a significant factor. The measurement mandrel material and geometry can work in conjunction with the sample bonding technique to create a dominant measurement variable: the axial strain of the conductor. Under a condition where (1) the circumferential thermal contraction of the measurement mandrel is greater than the axial thermal contraction of the conductor and (2) the bonding method creates a strong coupling between the sample and the measurement

mandrel, significant axial strain of the conductor at 4 K may result. This study discovered that the circumferential thermal contraction of the G-10 fiberglass-epoxy tubes used for the measurement mandrels depends on the tube's geometry, owing to its composite structure. In particular, the ratio of the tube wall thickness to its radius strongly affects its thermal contraction. Based on these observations, a systematic study was made of the effect of G-10 measurement mandrel geometry on the measured I_c .

For the measurement mandrel study, a glass-filled epoxy adhesive was used for bonding the sample to the mandrel. This technique insured the strong bond and rigid coupling between the sample and mandrel that is necessary for positive stress transmission.

Experimental Details

The Nb₃Sn wire measured in this study had a diameter of 0.68 mm with 37 sub-bundles, each contained 150 Nb filaments. The conductor fabrication method was an internal-tin diffusion process. A single diffusion barrier of Ta separated the filament region from the outer layer of Cu. The sample reaction temperature was 700°C for 48 h.

The measurement mandrels were constructed from G-10 tubes that had a cylindrical copper current contact rigidly attached to each end. Each contact had a superconductive bus bar (Cu and Nb₃Sn tape) connected to it. The sample was transferred from the reaction mandrel onto the measurement mandrel by carefully unthreading the sample from the reaction mandrel and slipping it onto the ungrooved measurement mandrel. The one current contact that was removed for this transfer was then reattached to the measurement mandrel and the sample was tightened onto the mandrel. Each end of the sample was then soldered onto its current contact. To avoid persistent currents, an effort was made to not have a complete superconductive loop formed by the sample and bus bar around the current contact. Three pairs of adjacent voltage taps were placed along the center of the sample. Each pair had a separation of about 10 cm and there was a 1 to 2 cm gap between adjacent pairs. The sample was bonded to the mandrel with glass-filled epoxy and allowed to cure. The epoxy coat was kept thin to enhance the heat transfer from the sample to the helium bath. This unit was then mounted in the test fixture where the electrical connections were completed.

The I_c measurements⁴ were made with forward (antiparallel magnetic fields, Lorentz force in) and reverse (parallel magnetic fields, Lorentz force out) current directions to determine the effect of self-field and sample-to-mandrel bonding (strain effect). Unless otherwise stated, the I_c values given are averages over all taps, observations, and current directions at an electric field strength criterion of 10 μ V/m. The precision of the I_c measurement was about $\pm 0.2\%$. A statement regarding the accuracy of these measurements is presently inappropriate because of the strong systematic effects of sample mandrels.

Another parameter that was determined during the I_c measurement is n . The parameter n is defined by the approximate voltage-current relationship,

$$V = V_0 (I / I_0)^n,$$

where I_0 is a reference I_C at a voltage criterion V_0 , V is the sample voltage, I is the sample current, and n reflects the shape of the curve with typical values from 20 to 60. A higher number means a sharper transition. A lower value of n can be an indication of sample damage or strain.

Results

Critical Current

A summary of the I_C data is given in Table I and in Fig. 1. The information contained in Table I is the I_C data, sample mandrel dimensions, and intercomparisons of I_C data. The I_C data are given at magnetic fields from 6 to 12 T. The effects of sample mandrel geometry and thermal cycling were studied. The column headings of Table I contain key words that relate to these variables. Each column, which is labeled with a letter from A to D, is a data set taken for a single thermal cycle. Specimens are numbered 1 and 2. Different data columns that are for the same specimens (columns A and B for example) indicate a thermal cycle where the specimen was measured at 4 K, warmed to room temperature, again cooled to 4 K, and remeasured. In some cases, the mounting configuration of the specimen was changed between these measurements (columns B and C for example). The sequence of the thermal cycles is from left to right in the table.

The key words heading the columns of Table I (thick, thin, and bored) are used to indicate the measurement variables. Thick and thin refer to the ratio of wall thickness to outer radius of the sample mandrel. Under the Sample Mandrel Dimensions section of the table, these specific values are listed for each data set. Bored refers to a specimen that was originally mounted and measured on a thick walled mandrel. The specimen was then brought to room temperature (thermally cycled) and the mandrel inner diameter was bored to a larger dimension, resulting in a reduced wall thickness. The specimen's I_C was then remeasured.

A comparison of the I_C data in columns A and B is a measure of the I_C variation due to thermal cycling. The maximum variation was 0.4% at 10 T (the highest magnetic field for column A) as shown in the intercomparison portion of the table ($(A-B)/B$). This small variation upon thermal cycling was representative of all observations. Column C was a special case of a thin walled mandrel in that it was bored (machined with the specimen mounted on the mandrel). Because this was the same specimen as A and B, the comparison is a systematic one. The intent of this procedure was to determine the effect of mandrel wall thickness on the measured I_C of a particular specimen. The intercomparison data ($(B-C)/C$) shows a strongly field-dependent variation of I_C (indicative of a strain effect) with a maximum difference of 40% at 12 T. This is thought to result from a change in the conductor pre-strain (at 4 K) due to variation in thermal contraction between thick- and thin-walled G-10 tubes. However, machining may have changed the mandrel's outer diameter at room temperature, due to stress relief, and, thus, the pre-strain state of the conductor. More details regarding thermal contraction of G-10 measurement mandrels and the resulting I_C degradation due to axial strain are presented below. The comparison between C and D showed only a small difference, 3 to 4%, with very little field dependence ($(C-D)/D$). This indicates that the effect of boring was about equivalent to that of simply mounting a specimen on a thin walled tube.

Figure 1 is a semilogarithmic plot of I_C versus magnetic field. This type of plot was used because

Table I. I_C Data and Mandrel Dimensions

Critical current (amperes) at 10 μ V/m				
Specimen	1 thick	1 thick	1 thin bored	2 thin
$\mu_0 H, T$	(A)	(B)	(C)	(D)
6	343.3	343.2	397.3	386.3
7	268.4	267.6	318.4	308.9
8	207.0	207.4	253.8	246.0
9	156.5	156.6	200.1	193.5
10	113.6	114.0	154.7	149.3
11		78.5	116.0	111.9
12		50.2	83.5	80.4

Sample Mandrel Dimensions				
	(A)	(B)	(C)	(D)
Wall, mm	9.3	9.3	2.5	2.0
Rad., mm	15.6	15.6	15.6	15.6
Wall/Rad	60%	60%	16%	13%

Intercomparison of Critical Current Data			
$\mu_0 H, T$	(A-B)/B	(B-C)/C	(C-D)/D
6	0.0%	-13.6%	2.8%
7	0.3%	-16.0%	3.1%
8	-0.2%	-18.3%	3.2%
9	-0.1%	-21.7%	3.4%
10	-0.4%	-26.3%	3.6%
11		-32.3%	3.7%
12		-39.9%	3.9%

it illustrates the percentage differences between the curves. The thick curve is significantly lower than the others. Figure 2 is a semilogarithmic plot of n versus magnetic field. The significant element of this plot is the lower values of n for the thick curve at the higher magnetic fields. This is consistent with a strain degradation.

Thermal Contraction

Thermal contraction measurements on NEMA (National Electrical Manufacturers' Association) G-10 glass-epoxy composites have been published for the plate

geometry^{5,6} but not for the tube geometry. The contraction of a G-10 plate is highly anisotropic. In the nomenclature of composites, the two directions in the plane of the fiberglass fabric are warp and fill. The direction perpendicular to the plane of the fabric is referred to as the normal direction. The thermal contraction from 293 K to 4 K is about 0.24% for the warp direction and 0.71% for the normal direction. The contraction in the fill direction is expected to be a little more than that of the warp direction. The contraction in the warp direction is dominated by the fiberglass fabric and the normal direction is dominated by the epoxy. The G-10 tubes used for measurement mandrels were rolled spirals of fiberglass fabric embedded in an epoxy matrix, rather than tubes machined from plate material. The radial direction for a rolled tube is normal to the fabric. The radial contraction of a tube is different than the contraction of a plate, however, because the circumferential fiberglass is put into hoop compression by the epoxy, and the resulting contraction is a competition between the two structural components. The dependence of the radial contraction on wall thickness is expected to be caused by this competition.

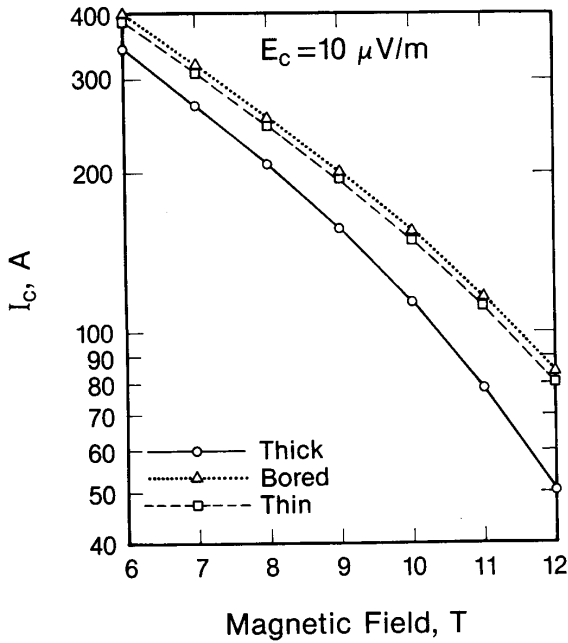


Figure 1. A semilogarithmic plot of I_c at an electric field criterion of $10 \mu\text{V/m}$ versus magnetic field.

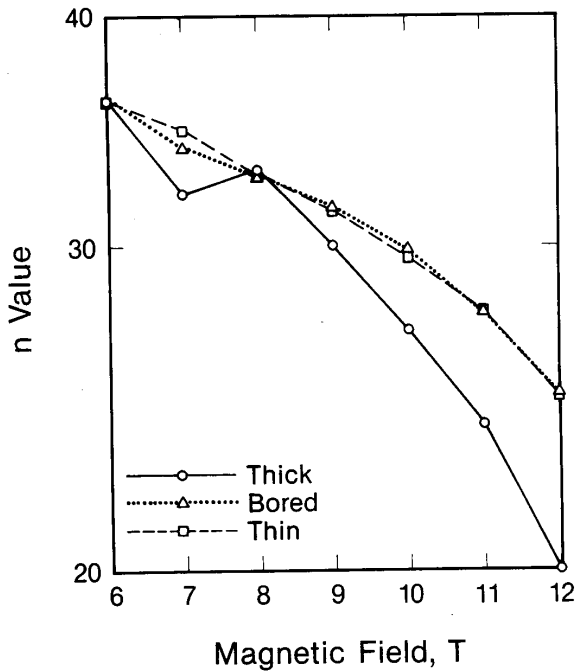


Figure 2. A semilogarithmic plot of n value versus magnetic field.

A thick-walled G-10 tube was originally selected as a common sample mandrel material to allow adaptation of one size tube to the various test fixtures used by the different laboratories. However, a thick-walled tube is difficult to manufacture without delaminations that can cause irregular contraction and voids when they are machined. Also, the outer diameter can change when the inner diameter is bored. Another observation was that the radial contraction can be slightly asymmetric; this will result in an approximately elliptical rather than circular cross section at low temperatures. In order to make an approximate correction for this, the thermal contraction measurements are the average of two approximately orthogonal measurements of the tube's diameter.

As briefly mentioned above, thermal contraction measurements were made on several G-10 tubes in order to estimate the resulting conductor strain. In the interest of expediency, these measurements were limited both in accuracy and precision; nonetheless, the measurements give an indication of the variation in thermal contraction between the tubes. These tests consisted of measuring the outside diameter of the G-10 tube at room temperature, submerging the tube in liquid nitrogen, allowing it to reach thermal equilibrium, and then quickly removing it and remeasuring the diameter. These measurements were made with a precision micrometer, but they were limited by the practical difficulties of the measurement.

The measurements showed a substantial difference between the radial thermal contraction of G-10 tubes with different wall thicknesses. The results of the thermal contraction measurements are shown in Table II. As indicated by the column headings in the right hand portion of the table, four different samples were measured. Of the four samples, the geometry of sample 1 was most like that of the actual measurement mandrels. This sample had a stepped cross-sectional geometry characterized by a longitudinal variation in its inner and outer diameters. The outside diameter of the sample was reduced at its ends and its inside diameter was enlarged at its center. This stepped geometry was necessitated by the cylindrical current contacts that were flush mounted over the ends of the mandrel. Reducing the outside diameter allowed the contacts to slip over the mandrel's ends; enlarging only the central portion of the mandrel's inside diameter allowed a reduction in the mandrel's wall thickness only in the area of the sample, while maintaining the required support in the area of the current contacts. The other three samples had constant inside and outside diameters along their lengths.

Table II. Thermal Contraction of G-10 Tubes

Mandrel Dimensions		Outer Diameter Thermal Contraction	
Ratio Wall/Radius	Wall Thickness	Sample 1 $\Delta d/d$	Sample 2 $\Delta d/d$
59%	9.27 mm	0.39%	0.41%
49%	7.70 mm	0.38%	0.36%
39%	6.10 mm	0.33%	0.32%
28%	4.32 mm	0.30%	0.28%
16%	2.54 mm	0.25%	0.23%
13%	2.03 mm	0.25%	0.24%
Ratio Wall/Radius	Wall Thickness	Sample 3 $\Delta d/d$	Sample 4 $\Delta d/d$
20%	3.18 mm	0.25%	
30%	4.76 mm		0.28%

Samples 1 and 2 were progressively bored to larger inside diameters while samples 3 and 4 had factory diameters (not machined) and were measured to test the equivalence between factory tubes and bored tubes with respect to thermal contraction.

For each sample, the table shows the tube's wall thickness, the ratio of the tube's wall thickness to its radius in percent, and the thermal contraction of the tube between room and liquid nitrogen temperatures ($\Delta d/d$). The data indicate that the thicker walled tubes contract more than the thinner ones. In addition, the good agreement between the data for samples 1 and 2 indicates that the contraction of the actual measurement mandrels is similar to that of simple tubes. The agreement of the data for samples 3 and 4 with those of 1 and 2 indicates that the bored tubes behave in a manner similar to that of factory tubes. Samples 1 and 2 with wall/radius ratios of 59%, 16%, and 13% have respectively similar dimensions to the thick, thin bored, and thin measurement mandrels of Table I.

A bias in this study exists as a result of the thermally transient measurement conditions (with a systematic difference in thermal mass) and the fact that it was conducted at liquid nitrogen, rather than liquid helium, temperature. Both of these factors result in an underestimate of the actual thermal contraction between room and liquid helium temperatures. Based on the temperature dependence of the thermal contraction of G-10 plate,⁵ the thermal contraction to 4 K was estimated as -0.28% for the thin walled mandrel and -0.48% for the thick walled mandrel. The thermal contraction of the Nb₃Sn conductor was only -0.21%. Consequently, the G-10 contraction may have introduced additional amounts of conductor pre-strain. The amount of compressive pre-strain might depend on several factors including the mandrel's wall thickness and the strength of the mandrel-to-conductor bond.

Considerable I_c tensile-strain-sensitivity data were available for this sample; however, no explicit data were available for compressive strain sensitivity.

Consequently, the strain scaling law,³ in conjunction with the available tensile strain data, was used to estimate the expected I_c degradation for compressive strain. The results of these calculations predict a -33% reduction in the I_c at 12 T for the thick-walled specimens as compared to the thin-walled ones; the observed reduction was -40%. These measurements and calculations are only approximate, but the trend is apparent. In all cases, the thick walled samples had reduced I_c 's and this reduction was in approximate agreement with that predicted by the strain scaling law.

Conclusions

The bonding method and the mandrel material and geometry have a significant effect on the critical current measurement of Nb₃Sn. Thick-walled G-10 tubes contract about 0.2% more than thin-walled G-10 from room to liquid helium temperature. Thus, the amount of differential thermal contraction between the mandrel and the sample depends on the wall thickness of the G-10. The effect of strain on the I_c of a particular sample depends on its upper critical field. The sample tested here has an upper critical field of -19 T and the difference between critical current measurements on thick- and thin-walled G-10 was about 40% (predicted 33%) at 12 T. Another sample with an upper critical field of -24 T was also measured and, in this case, the difference between critical current measurements on thick- and thin-walled G-10 was about 17% (predicted 24%) at 12 T.

G-10 tubes that have diameters similar to that of those tested, and wall thicknesses about 20% or less of the tube's radius, are well matched in thermal contraction to Nb₃Sn wires and use of this type of tube for measurement mandrels should result in a minimum of conductor strain. The scaling of this effect for tubes of various diameters has not been demonstrated, but scaling is probably accurate for a limited range of tube diameters.

Acknowledgments

The authors extend their thanks to J. W. Ekin for discussions on these results; to R. M. Folsom for sample preparation, data reduction, and plotting; to D. L. Rule for help with data plotting; to W. E. Look for assistance with the magnetic field calibration; and to the other VAMAS participants.

This work was supported by the Department of Energy, Office of Fusion Energy and Division of High Energy Physics.

An effort was made to avoid the identification of commercial products by the manufacturer's name or label, but in some cases these products might be indirectly identified by their properties. In no instance does this identification imply endorsement by the National Bureau of Standards, nor does it imply that the products are necessarily the best available for that purpose.

References

- [1] L. F. Goodrich and F. R. Fickett, "Critical Current Measurements: A Compendium of Experimental Results," Cryogenics, vol. 22, pp. 225-241, May 1982.
- [2] Standard Test Method for D-C Critical Current of Composite Superconductors, Annual Book of ASTM Standards, ASTM B714-82, Part 02.03, pp. 595-98, American Society for Testing and Materials, Philadelphia, PA (1983).
- [3] J. W. Ekin, "Strain Scaling Law for Flux Pinning in Practical Superconductors. Part 1: Basic Relationship and Application to Nb₃Sn Conductors," Cryogenics, vol. 20, pp. 611-624, Nov. 1980.
- [4] L. F. Goodrich, "Development of Standards for Superconductors, Interim Report January 1986 - December 1987," NBSIR 88-3088, National Bureau of Standards, Boulder, CO (February 1988).
- [5] G. Fujii, J. W. Ekin, R. Radebaugh, and A. F. Clark, "Effect of Thermal Contraction of Sample Holder Material on Critical Current," Adv. Cryog. Eng.-Materials, vol. 26, pp. 589-598, Plenum Press, New York (1980).
- [6] A. F. Clark, G. Fujii, and M. A. Ranney, "The Thermal Expansion of Several Materials for Superconducting Magnets," IEEE Trans. Mag., MAG-17, 2316, 1981.